PAPER Special Section on Photonic Network Technologies in Terabit Network Era

Compact Matrix-Switch-Based Hierarchical Optical Path Cross-Connect with Colorless Waveband Add/Drop Ratio Restriction

Ryosuke HIRAKO[†a)], **Kiyo ISHII**[†], ***Student Members***, **Hiroshi HASEGAWA**[†], ***Senior Member***, **Ken-ichi SATO**[†b)], ***Fellow***, ***and*** **Osamu MORIWAKI**[††], ***Member***

SUMMARY We propose a compact matrix-switch-based hierarchical optical cross-connect (HOXC) architecture that effectively handles the colorless waveband add/drop ratio restriction so as to realize switch scale reduction. In order to implement the colorless waveband add/drop function, we develop a wavelength MUX/DMUX that can be commonly used by different wavebands. We prove that the switch scale of the proposed HOXC is much smaller than that of conventional single-layer optical cross-connects (OXCs) and a typical HOXC. Furthermore, we introduce a prototype system based on the proposed architecture that utilizes integrated novel wavelength MUXs/DMUXs. Transmission experiments prove its technical feasibility.

key words: *hierarchical optical cross-connect, waveband, add/drop ratio, MUX/DMUX, AWG*

1. Introduction

Broadband access using xDSL and FTTx is being rapidly adopted throughout the world. In order to support the expected further traffic expansion caused by future services such as super-/ultra- high definition TV (6G/72G bps/channel, uncompressed) and video on-demand services, hierarchical optical path networks that utilize waveband paths (bundles of wavelength paths) have been investigated [1]–[3].

Significant endeavours have been made to develop efficient design algorithms for hierarchical optical path networks; the aim is to reduce total network cost. In most evaluations, the cost is approximated by a linear function of the number of switch ports and links. Recent advances [4]–[8] have revealed that significant cost reductions can be achieved with hierarchical optical path networks, compared to single-layer optical path networks, over a wide range of network parameter values.

Hierarchical optical path cross-connects (HOXCs) consist of waveband path cross-connects (WBXCs) and wavelength path cross-connects (WXCs) that manage two different path granularities. The switch scale reduction attained by HOXCs depends on the waveband add/drop ratio [9], the ratio of the number of added/dropped waveband paths to that of all incoming/outgoing waveband paths. The waveband add/drop ratio restriction can be defined in two ways; restricting the number of waveband paths in each waveband index and restricting the number of all waveband paths. Imposing an upper bound on the former is called here the add/drop ratio restriction on each waveband, while that for the latter is called the colorless waveband add/drop ratio restriction. HOXC architectures [10] based on the wavelength selective switch (WSS) [11], [12] and waveband selective switch (WBSS) [13] can naturally implement the former restriction. Matrix-switch [14], [15]-based HOXC architectures can implement both restrictions [9]. It is desirable to minimize network cost, or to minimize number of cross-connect ports and links, while suppressing the waveband add/drop ratio to minimize switch scale. Recently developed network design algorithms [16]–[18] attain this optimization when we introduce these restrictions. Since the colorless add/drop restriction is less stringent than the other from the network design point of view, applying the colorless restriction to the HOXC leads to a simultaneous reduction in cross-connect switch scale and port count [16]–[18]. In this paper, we focus on the matrix-switch-based HOXC architectures that can support the colorless waveband add/drop ratio restriction. Another important point to be mentioned regarding the matrix-switch-based architecture approach is its proven effectiveness in the ring connecting node application. It has been shown that the matrix-switch-based HOXC can reduce switch scale by more than 70%, compared to the single-layer OXC architecture [19]. It should also be noted that the micro-optic technology-based WSS has wider passband than the PLC (Planar Lightwave Circuit)-based wavelength MUX/DMUX and hence can realize smaller WSS crosstalk. However, it has been recently verified that digital coherent technologies can greatly mitigate the crosstalk requirement [20], and hence their application can substantially relax the requirements imposed on passband width or filter shape.

We propose in this paper a novel compact matrix-switch-based HOXC architecture that supports the colorless waveband add/drop ratio restriction. To implement the colorless operation, we invented a novel colorless wavelength MUX/DMUX that can be commonly utilized by all waveband paths regardless of their waveband index. We have

Manuscript received August 31, 2010.
Manuscript revised December 3, 2010.
[†]The authors are with Nagoya University, Nagoya-shi, 464-8603 Japan.
[††]The author was with NTT Photonics Laboratories, NTT Corporation, Atsugi-shi, 243-0198 Japan.
a) E-mail: r_hirako@echo.nuee.nagoya-u.ac.jp
b) E-mail: sato@nuee.nagoya-u.ac.jp
DOI: 10.1587/transcom.E94.B.918

demonstrated that the proposed HOXC can greatly reduce switch scale compared to the conventional HOXC [9]. A prototype HOXC is constructed on the newly developed devices. The devices include multiple colorless wavelength MUXs/DMUXs that are compactly and monolithically implemented on a PLC chip, and specially designed matrix switches having additional input/output ports for colorless add/drop operations. We verify the performance of the prototype HOXC: a cascade of 5 HOXC nodes, including one grooming operation, has a power penalty (BER=10^{-9} at 10 Gbps) of less than 0.2 dB. A preliminary report on this HOXC has been presented at an international conference [21].

2. Waveband Add/Drop Ratio Restriction

To realize the economical introduction of large scale optical cross-connects and the dynamic routing of optical paths, a sufficiently flexible add/drop capability and reduced switch scale must be realized simultaneously. As mentioned before, the switch scale of a hierarchical optical cross-connect depends on the parameter called the waveband add/drop ratio [9]. Two different restriction schemes are defined as follows.

1) *Add/Drop Ratio Restriction on Each Waveband:* For an HOXC node, let the number of added/dropped waveband paths in the i-th waveband be $b^{(i)}_{add/drop}$ and that of outgoing/incoming waveband paths to/from the other nodes be $b^{(i)}$. Then, for the given upper bound on add/drop ratio on each waveband, α_{each}, the HOXC node must satisfy

$$\max_{b^{(i)}\neq 0} \frac{b^{(i)}_{add/drop}}{b^{(i)}} \leq \alpha_{each}.$$

2) *Colorless Waveband Add/Drop Ratio Restriction:* This add/drop ratio restriction, $\alpha_{colorless}$, is valid for all the wavebands and is expressed as,

$$\frac{\sum_i b^{(i)}_{add/drop}}{\sum_i b^{(i)}} \leq \alpha_{colorless}.$$

The number of optical ports in the network may need to be increased if the constraint on add/drop capability is tight. A recent work [16], [17] proved that a network that complies with the colorless add/drop restriction can be constructed with almost the same number of optical cross-connect ports as the network without any restriction, if the restriction related to grooming is not so tight, say, less than 0.2. Further explanations on this are given in Sect. 6.

This paper proposes a novel HOXC architecture that can satisfy the colorless waveband add/drop ratio restriction very effectively.

3. Conventional Node Architectures

Let K be the number of incoming/outgoing fibers, M the number of waveband paths per fiber, N the number of wavelength paths per waveband, L the number of wavelength paths per fiber, i.e. $L = MN$. We take x as the upper bound of ratios of added/dropped wavelength paths to all incoming/outgoing wavelength paths (wavelength add/drop ratio) for a single layer OXC. Similarly, let y and z be the upper bounds for waveband add/drop ratio and wavelength add/drop ratio for a waveband path cross-connect (WBXC) and wavelength path cross-connect (WXC) in the HOXC, respectively. Hereafter, we assume that $x = y$ and $z = 1$ since these values maximize switch scale reduction in the HOXC [9].

3.1 Evaluation of Switch Scale

In the rest of this paper, we take the number of equivalent 1×2 element optical switches as the metric used to evaluate total switch complexity. For example, an $N \times N$ matrix switch is regarded as a set of N^2 1×2 switches.

3.2 Conventional Single-Layer OXC Node Architecture

In this section, we review two conventional single-layer OXC architectures. In single-layer OXCs, wavelength paths are demultiplexed by DMUXs, routed by WXCs, and then combined by MUXs. Wavelength converters can be utilized to avoid wavelength collision, but this paper does not discuss the implementation of this costly device. Even when the node does not have any converters, it has been verified that wavelength collision can be effectively mitigated by adopting effective optical path routing algorithms [7], [22].

We can classify the non-blocking characteristics into 3 types; strictly non-blocking, non-blocking in a wide sense, and rearrangeably non-blocking [23], [24]. If any input can always be connected in any viable way to any unused output without disturbing existing connections, the switch is strictly non-blocking. Hereafter, we restrict our attention to non-blocking switches.

Figures 1 and 2 show two single-layer OXCs. Considering the reduction of switch scale, we assume that the number of add/drop ports is less than that of ports for incoming/outgoing paths, namely $x < 1$.

Figure 1 shows a single-layer OXC consisting of a single large matrix switch, which can connect optical paths

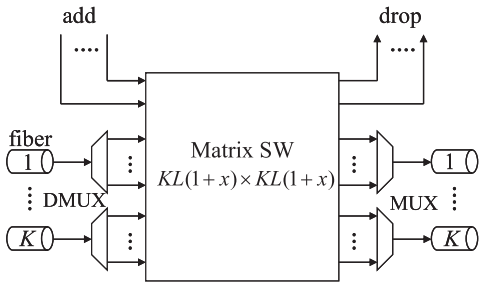

Fig. 1 Single-layer OXC with a large matrix switch (type S1).

from any input or add port to any output or drop port. Therefore, it realizes the most flexible add/drop capability that can add/drop any combinations of wavelength paths. We call this single-layer OXC type S1.

Figure 2 shows a single-layer OXC where a matrix switch is divided into small switches dedicated to each wavelength. Although switch scale is reduced, the number of added/dropped paths is, for each wavelength, bounded by x and hence the added/dropped restriction is more stringent than that in type S1. We call this single-layer OXC type S2.

3.3 Conventional HOXC Node Architecture [9]

A conventional HOXC architecture [9] with colorless waveband add/drop ratio restriction is shown in Fig. 3. We call this HOXC type H1. The HOXC architecture consists of $2K \times 2K$ matrix switches, each of which is dedicated to one waveband, two $KM \times yKM$ matrix switches, which restrict the number of added/dropped wavebands, and a WXC with a single large $yKMN(z+1) \times yKMN(z+1)$ matrix switch. Thanks to the $KM \times yKM$ matrix switches, the configuration satisfies the colorless add/drop restriction.

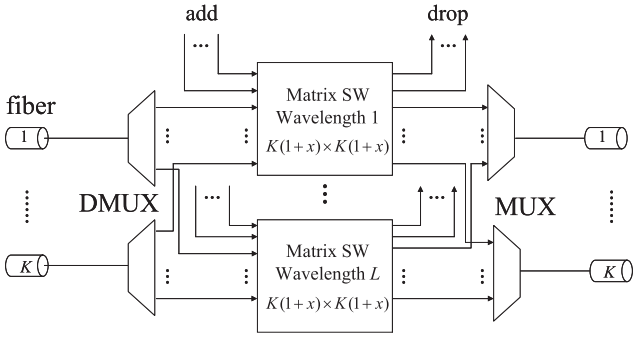

Fig. 2 Single-layer OXC that consists of matrix switches dedicated to the same-wavelength paths (type S2).

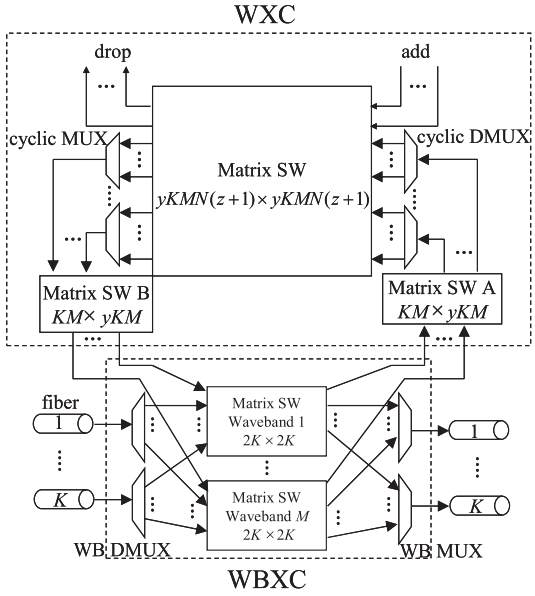

Fig. 3 Conventional HOXC architecture (type H1).

The colorless waveband add/drop capability requires each MUX/DMUX in WXC to be able to multi-/demultiplex any waveband path with different waveband indexes. That is, regardless of waveband index, it must be possible to freely distribute wavelength paths in a waveband to the output ports of the DMUX where the number of ports equals that of wavelength paths. However, the architecture is possible only with the continuous waveband arrangement (discussed in Sect. 5) and requires cyclic AWGs in WXC part. The switch scale reduction has been analyzed [9] and a large matrix switch is necessary for realizing the colorless wavelength add/drop capability in the WXC part. The relatively large switch scale is an issue to be resolved.

4. Proposed HOXC Node Architecture

Our strategy for reducing switch scale is to divide a common-purpose large switch into as many small dedicated-purpose switches as possible. If, for example, a 16×16 switch can be divided into four 4×4 switches dedicated to the different functions, the switch scale (total number of cross-points) can be reduced by 75%. Thus, if we can attain the desired switching functions, the total switch scale can be reduced. Given this aim, we have developed a colorless wavelength MUX/DMUX that uses multiple small-scale switches instead of a large common switch in the WXC part.

Figure 4 shows the proposed HOXC architecture. Hereafter, we call this HOXC type H2. WBXC part consists of multiple $K \times K$ matrix switches, each of which is dedicated to one waveband, and separate $K \times yKM$ matrix switches, which select waveband paths to be added/dropped in each waveband. Note that the latter switches are connected in parallel to each MUX/DMUX in WXC. WXC part consists of $yKM \times yKM$ matrix switches where the i-th switch is shared by the i-th wavelength paths in incoming wavebands, and 1×2 matrix switches attached to all input

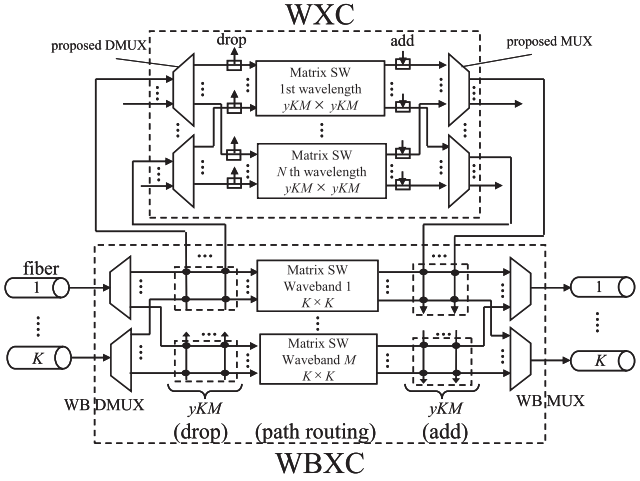

Fig. 4 Proposed HOXC architecture (type H2).

and output ports in $yKM \times yKM$ matrix switches. The major differences from the conventional HOXC in Sect. 3.3 are; 1) WXC consists of N smaller matrix switches where the i-th switch is shared by the i-th wavelength paths in incoming wavebands, 2) a novel MUX/DMUX that can be used by any waveband is introduced to achieve efficient colorless waveband add/drop capability, 3) the proposed WBXC replaces two matrix switches (Matrix SW A and B in Fig. 3) between WBXC/WXC that are necessary to attain colorless operation in conventional HOXC by two separate sets of matrix switches that are located before and after each $K \times K$ matrix switch for waveband index i. Details of MUX/DMUX, one of the key devices in creating the proposed HOXC, are presented in the next section.

5. Colorless Wavelength Multi-/Demultiplexer

We assume a given set of wavelengths, $\{\lambda_1, \lambda_2, \ldots, \lambda_{NM}\}$, is equally divided into M wavebands, i.e. groups of wavelengths. Two typical waveband arrangements have been proposed [2]; continuous waveband arrangement (Fig. 5(a)) and interleaved waveband arrangement (Fig. 5(b)). In the former, the set of wavelengths is divided into M wavebands as $\{\lambda_{iN+1}, \lambda_{iN+2}, \ldots, \lambda_{(i+1)N}\}$ $(i = 0, 1, \ldots, M-1)$. In the latter, the set of wavelengths is divided into M wavebands as $\{\lambda_{i+1}, \lambda_{i+M+1}, \ldots, \lambda_{i+M(N-1)+1}\}$ $(i = 0, 1, \ldots, M-1)$. As discussed in the previous section, we must develop a device that can demultiplex the N wavelength paths of each waveband path into N output ports, each of which are fixed to one wavelength index regardless of the input waveband index. We realize this function utilizing an AWG-based device. Figures 6(a) and 7(a) show the newly proposed devices intended for the continuous and interleaved waveband arrangements, respectively. The necessary AWG input and output port number is $(MN - N + 1) \times (MN - N + 1)$ and $(MN - M + 1) \times (MN - M + 1)$ for continuous and interleaved waveband arrangement, respectively. Here we assume non-cyclic AWGs for simplicity, but we can also apply cyclic AWGs. Note that each can be used by any different waveband path, provided the input port of each waveband is fixed: wavebands input to each corresponding input port of the device are demultiplexed into the same fixed set of output ports. Please note that a single input waveband signal is delivered to each MUX/DMUX through WBXC drop switches.

As seen in Figs. 6(a) and 7(a), only a limited number of input/output ports of the AWG are utilized, in other words, many of the ports are left unused. To exploit these unused ports, we developed a simple method to integrate multiple colorless wavelength MUXs/DMUXs onto one AWG chip. We explain the schemes for the interleaved waveband arrangement. First, we assume that waveband set #1 (each waveband set consists of M wavebands) is connected to input port set $\{1, 2, \ldots, M\}$, the wavelengths of the waveband set are demultiplexed to output port set $\{BM + B - M, BM + B, \ldots, MN + BM + B - 2M\}$. Second, we connect waveband set #2 to input port set $\{M+2, M+3, \ldots, 2M+1\}$ that is shifted by $M+1$ ports from the input port set of waveband set #1. Then the output port set is $\{BM + B - 2M - 1, BM + B - M - 1, \ldots, MN + BM + B - 3M - 1\}$; it does

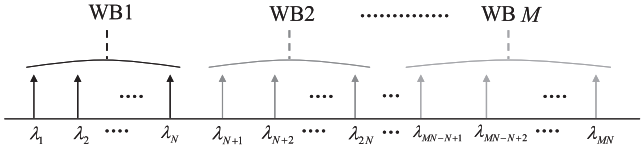

(a) Continuous waveband arrangement

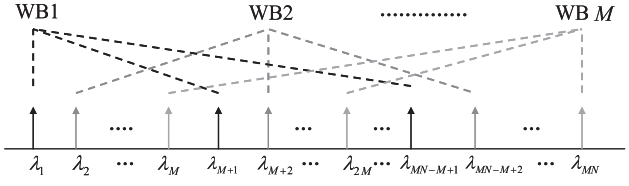

(b) Interleaved waveband arrangement

Fig. 5 Two waveband arrangements.

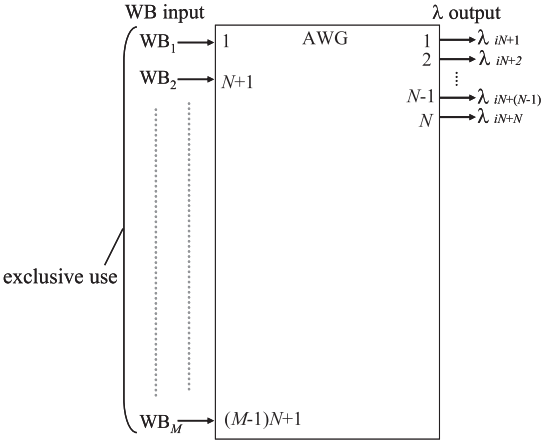

(a) Input ports arranged as single MUX/DMUX

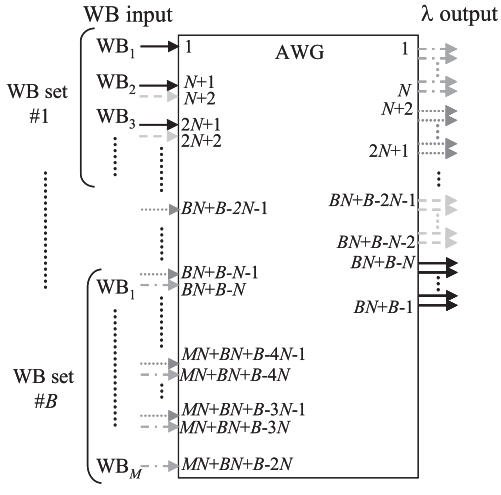

(b) Integration of multiple MUXs/DMUXs

Fig. 6 Integration of multiple MUXs/DMUXs onto an AWG (for continuous waveband arrangement).

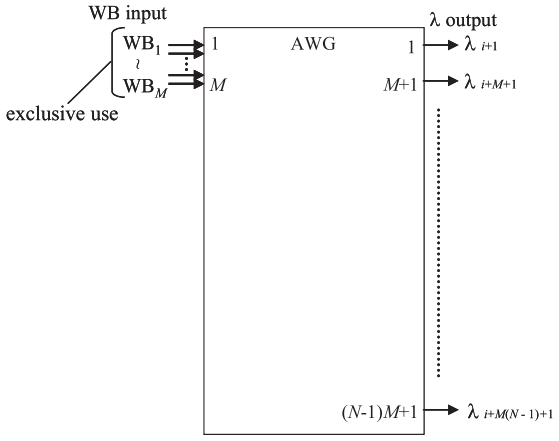

(a) Input ports arranged as single MUX/DMUX

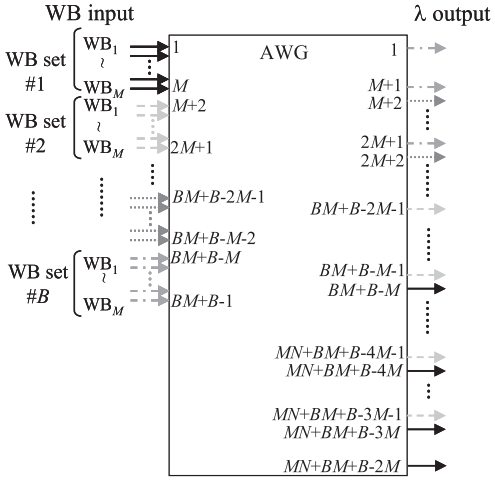

(b) Multiple MUXs/DMUXs

Fig. 7 Integration of multiple MUXs/DMUXs onto an AWG (for interleaved waveband arrangement).

not overlap waveband set #1. In order to integrate multiple colorless wavelength MUXs/DMUXs onto a single AWG efficiently, there are two requirements to be satisfied; 1) The input and output ports of each MUX/DMUX must not overlap, and 2) The interval between each waveband set should be minimized. If the input port set of waveband set #2 is shifted by equal to or less than M ports, requirement 1) is not satisfied. When the shift is by M+1 ports, requirements 1) and 2) are met for the first time. By repeating this operation, we can integrate multiple colorless wavelength MUXs/DMUXs onto a single AWG efficiently. As a result, port set $\{M+1, 2M+2, \ldots, \}$ on the left side of the AWG is left unused. This scheme can be easily extended to support the continuous waveband configuration. In the case of a continuous waveband arrangement, if the input port set of wavebands is shifted by equal to or less than N ports, requirement 1) is not satisfied. When the shift is by N+1 ports, requirements 1) and 2) are met for the first time. By repeating the operation of shifting input waveband port set by N+1 ports, we can integrate multiple colorless wavelength

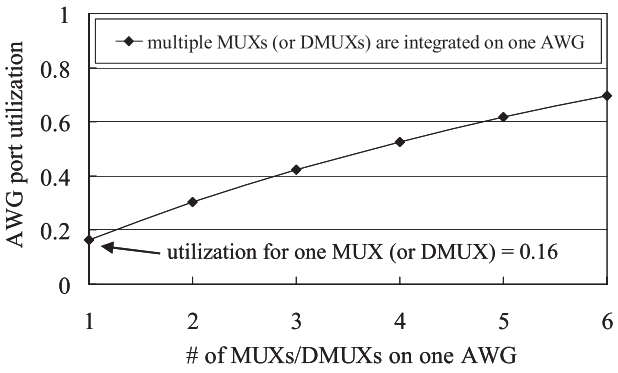

Fig. 8 AWG port utilization (for interleaved waveband arrangement).

MUXs/DMUXs onto a single AWG efficiently. Figures 6(b) and 7(b) show the proposed integrated devices for continuous and interleaved wavebands, respectively. Each device accommodates B sets of wavebands and the necessary input/output port numbers are $(MN + BN + B - 2N) \times (MN + BN + B - 2N)$ and $(MN + BM + B - 2M) \times (MN + BM + B - 2M)$ for continuous and interleaved waveband arrangements, respectively. These arrangements greatly enhance the utilization of AWG input and output ports. To confirm the effectiveness of the proposed integration method, we evaluated the AWG port utilization using the ratio of the number of ports utilized by MUXs/DMUXs to that of all AWG ports. Figure 8 shows a comparison of AWG port utilization rates. For the interleaved waveband arrangement, with $M = 4$, $N = 16$, the AWG port utilization rate for a single AWG colorless wavelength MUX/DMUX is 16%, and 70% when six MUXs/DMUXs are integrated onto a single AWG. The integrated arrangement reduces device footprint and hence cost. Similar results can be obtained for the continuous waveband arrangement.

6. Comparison of Switch Scale

In this section, we analyze the switch scale of the four OXC architectures discussed in the previous sections. Their characteristics are summarized in Table 1. Formulations of switch scale for each architecture are summarized in Table A· 1 in the Appendix.

Here switch scale is evaluated by necessary number of 1×2 element optical switches. Assumed parameter values are; $K = 10$, $M = 4$, $N = 16$, $L = 64$. Please note that the maximum number of input or output fibers for current optical cross-connects is 10 (=K), the number of wavelengths (=L=MN) per fiber of current WDM systems ranges from 40 to 96, so we assumed the MN value of 64. The typical number of wavelength paths per waveband is 16 (=N), a value that ensures the realization of the substantial benefits possible with the introduction of wavebands [7]. Figure 9 shows analyzed switch scale plotted on a logarithmic scale for the four OXCs. It shows that the single-layer OXC and HOXC architectures, type S1 and type H1, that adopt large matrix switches require much

Table 1 Comparison of single-layer and hierarchical OXCs.

XC type	WBXC structure	WXC structure	Add/Drop capability in WBXC
Conventional single OXC (type S1)	———	Single matrix SW	———
Conventional single OXC (type S2)	———	Independent SW is assigned to each wavelength	———
Conventional HOXC (type H1) [9]	Independent SW is assigned to each waveband	Single matrix SW	The number of added/dropped paths is limited on all wavebands
Proposed HOXC (type H2)		Independent SW is assigned to *i*-th wavelength in wavebands	

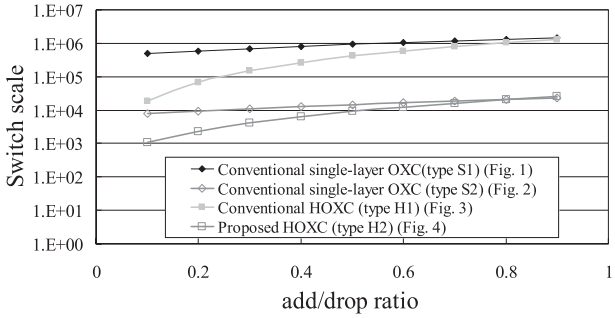

Fig. 9 Switch scale evaluation (from Figs. 1, 2, 3, and 4).

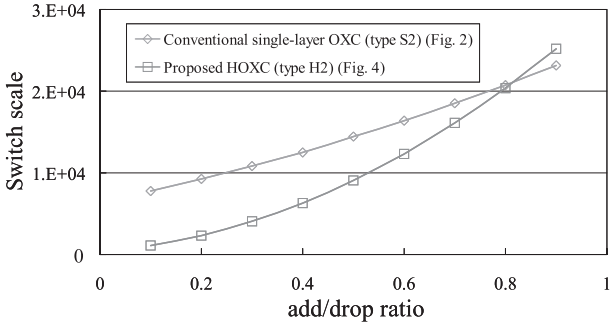

Fig. 10 Switch scale evaluation (from Figs. 2 and 4).

larger scales. It should be noted that these switch architectures allow colorless/contentionless/directionless optical path add/drop capabilities [25]–[27] that are useful for dynamic optical path operations. The flexibility can be attained not only with large matrix type optical switches, but also with electrical switches including simple matrix type electrical switches [28], and SDH/SONET and ODU cross-connects [29]. The introduction of electrical equipment requires additional intra-office optical links, which are much less expensive than transponders used for inter-office transmission, between electrical switches and client node systems such as routers. The electrical cross-connect may be required from the service point of view to attain sub-lambda granularities [30]. Figure 10 plots switch scale on a linear scale for the two other architectures, type S2 and type H2. For these architectures, additional mechanisms are necessary to attain colorless/contentionless/directionless optical path add/drop capabilities, but various solutions including electrical technologies exist [28], [30] as mentioned above. We, therefore, focus on the switch functions that are necessary to cross-connect optical paths that traverse the node. In Fig. 10, when $x = y = 0.2$, the proposed HOXC architecture has 75% smaller switch scale than the single-layer OXC's. Please note that the single-layer OXC architecture, type S2, imposes a tighter add/drop ratio restriction that is defined for each wavelength, while the proposed HOXC only imposes a colorless waveband add/drop ratio restriction, which allows any combination of waveband paths to be added/dropped.

Regarding add/drop ratio values, recent studies revealed that in a network that utilizes waveband routing, the waveband add/drop ratio required for wavelength path grooming can be so small, say 0.2, that it virtually does not increase total network cost when an appropriate network design algorithm is utilized that can optimize the network considering the add/drop ratio restriction [16]–[18], [31]. In other words, the use of small-scale wavelength-grooming switches (WXCs) in HOXC was shown to offer a new approach to the creation of optical networks that accommodate a large number of optical paths [31]. Particularly in this regard, the proposed HOXC (type H2) is proven to be very effective.

7. Development of Prototype HOXC System and Transmission Experiment

7.1 Integrated Colorless Wavelength MUX/DMUX

We implemented the proposed colorless wavelength MUXs/DMUXs with interleaved waveband arrangement on a number of 40×40 AWGs, each of which was equipped with one MUX and one DMUX for experimental simplification. Forty 100-GHz spaced channels ($191.7 + 0.1 \times n$ THz; $n = 0$–39) on an ITU-T grid were used. The 40 wavelengths were divided into five WBs, each of which consisted of 8 channels. Figure 11 shows a typical example of the transmittance of two (one MUX and one DMUX) integrated colorless wavelength MUX/DMUX. Figure 12 shows the insertion loss of a colorless wavelength MUX/DMUX. The insertion loss increased by about 1 dB for 8th-wavelength path of each waveband, but the maximum loss was less than 6 dB.

7.2 Prototype HOXC

Figure 13 shows the developed HOXC prototype that ac-

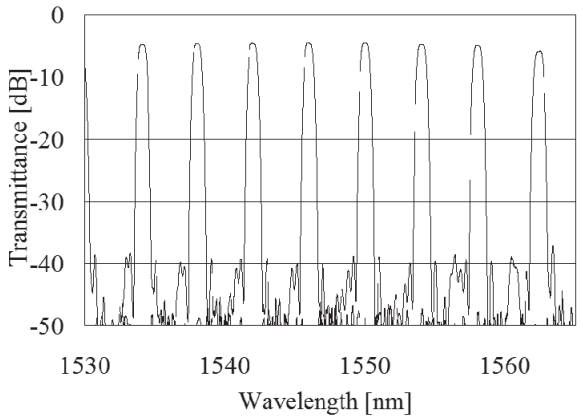

Fig. 11 Transmittance of two integrated colorless wavelength MUX/DMUX.

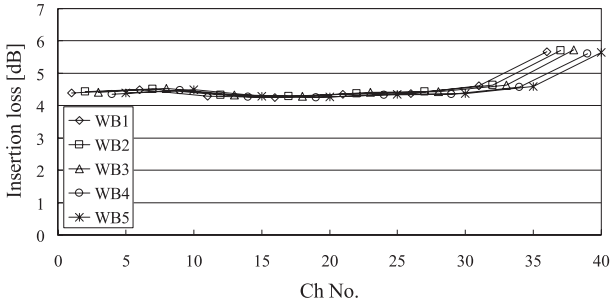

Fig. 12 Insertion loss.

commodates 8-input and 8-output fibers (degree 8). It consists of thirteen 8 × 8 matrix switches, ten 16 × 16 matrix switches with 16 through ports, four 4-arrayed 1 × 5 waveband MUXs/DMUXs, and eight integrated 40 × 40 cyclic AWGs (each accommodates both colorless wavelength MUX and DMUX). The waveband add/drop ratio is set at 0.2.

7.3 Transmission Experiment

Figures 14(a) and (b) show two examples of the output spectrum of the developed HOXC when signals are input from fiber #1; WB1, WB3, and WB5 are routed to output port 1 and WB2 and WB4 are to output port 2 as intended.

We assessed the transmission characteristics of two typical path configurations as shown in Fig. 15: (a) optical path was set between source and destination node pairs using direct end-to-end waveband, and (b) optical path with intermediate grooming. BER and power penalty were measured at each measurement point from (i) to (v) in Fig. 15. The experimental setup used is shown in Fig. 16 where the five boxes, #1 to #5, stand for the HOXC nodes in Fig. 15. Figures 17(a) and (b) show the evaluated BER. Figure 17 verifies that the BER performance degradation imposed by HOXC node traversal is very small. Figures 18(a) and (b) plot the power penalty at the BER of 10^{-9} versus the number of HOXC hops. With and without intermediate groom-

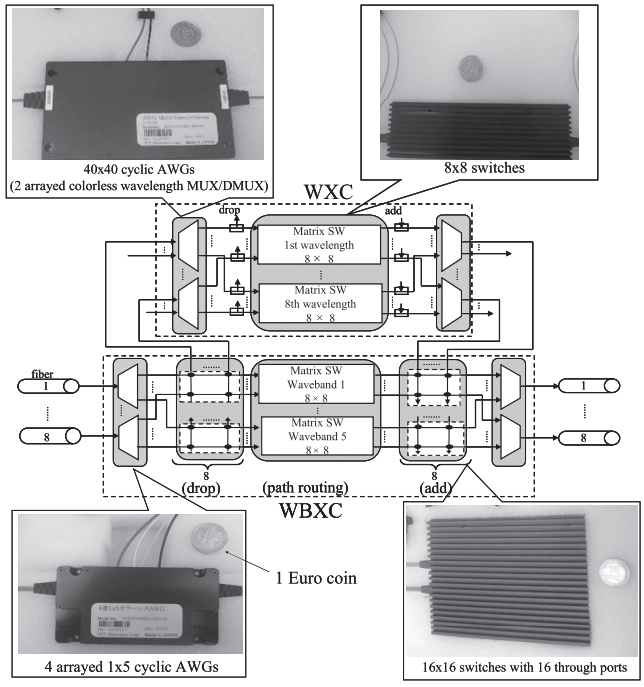

Fig. 13 Developed prototype HOXC architecture.

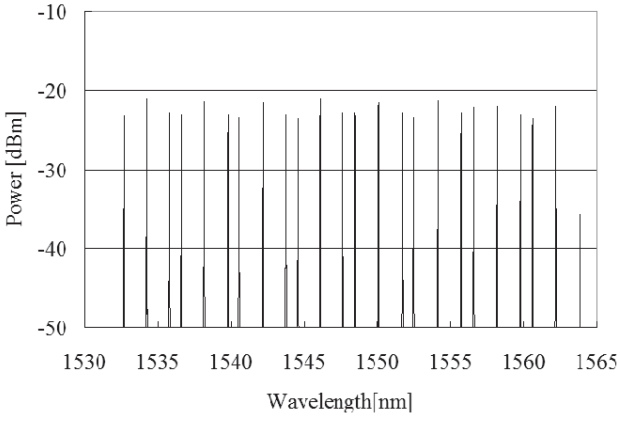

(a) Output port 1 (WB1, WB3, WB5)

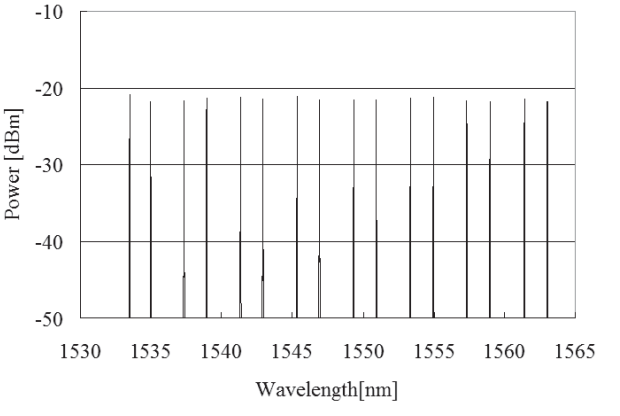

(b) Output port 2 (WB2, WB4)

Fig. 14 Output channel spectra (Input port 1).

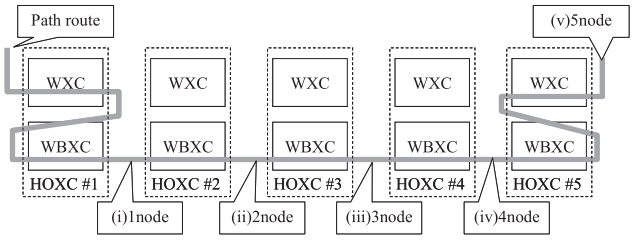

(a) End-to-End connection

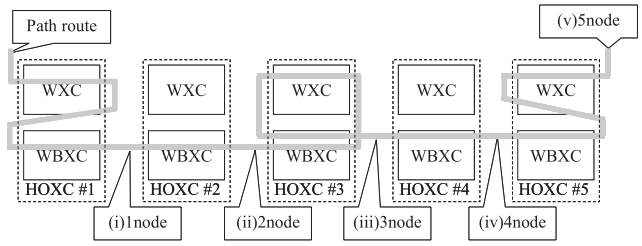

(b) With one time intermediate grooming

Fig. 15 Transmission testbed.

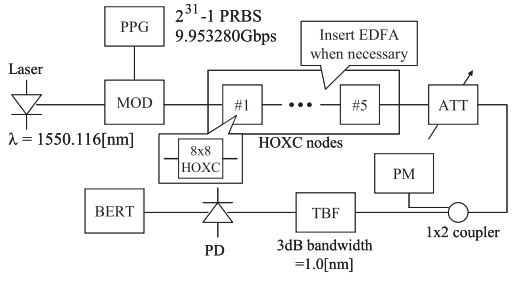

Fig. 16 Experimental setup for BER evaluation.

ing, power penalties were less than 0.2 dB after traversing 5 nodes. The slight reduction in power penalty at node 5 in Fig. 18 may be due to the experimental condition (i.e. light reflection from fiber connectors) or by measurement error.

8. Conclusion

We proposed a novel compact HOXC architecture that supports the colorless waveband add/drop ratio restriction. To implement this architecture, we developed the colorless wavelength MUX/DMUX, which can be commonly used by any waveband path. We verified the compactness of the proposed HOXC through switch scale evaluations including comparisons against conventional OXC architectures. A prototype system that used integrated multiple colorless wavelength MUXs/DMUXs was demonstrated. Transmission experiments confirmed the technical feasibility of the proposed HOXC system. This HOXC will play an important role in creating cost-effective large bandwidth networks.

Acknowledgment

This work is partly supported by CREST (JST).

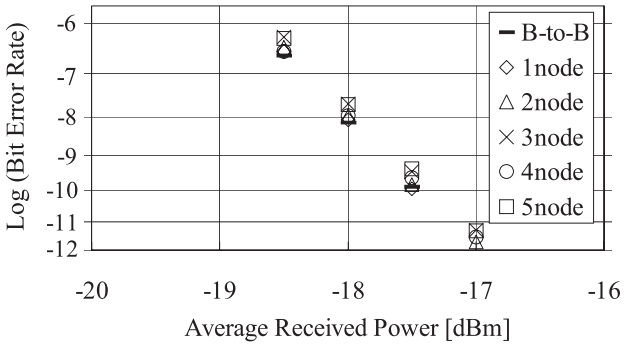

(a) End-to-End connection

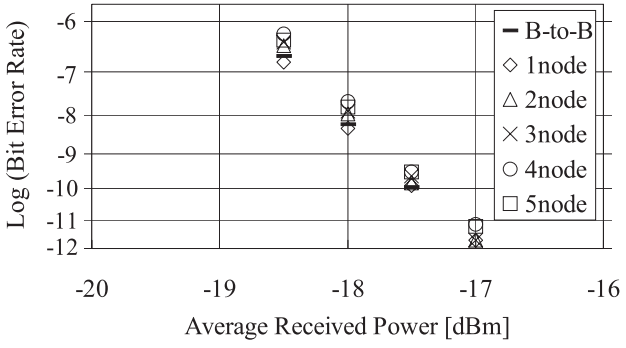

(b) With one time intermediate grooming

Fig. 17 Measured BER.

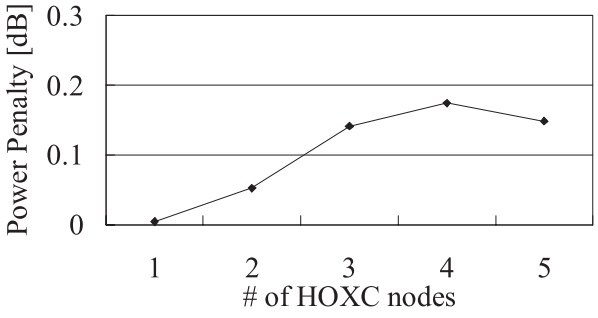

(a) End-to-End connection

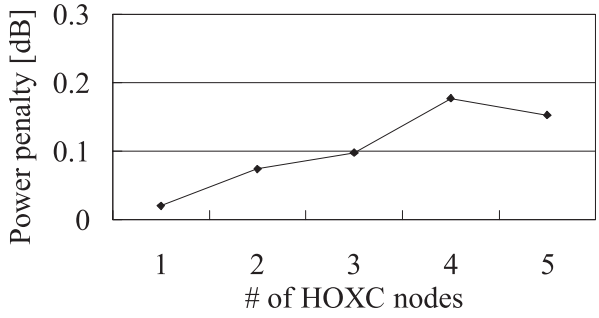

(b) With one time intermediate grooming

Fig. 18 Power penalty.

References

[1] L. Noirie, M. Vigoureux, and E. Dotaro, "Impact of intermediate

traffic grouping on the dimensioning of multi-granularity optical networks," Proc. Opt. Fiber Commun. Conference and Exposition and The National Fiber Optic Engineers Conf., pp.TuG3/1–3, March 2001.

[2] K. Sato and H. Hasegawa, "Prospects and challenges of multilayer optical networks," IEICE Trans. Commun., vol.E90-B, no.8, pp.1890–1902, Aug. 2007.

[3] K. Sato and H. Hasegawa, "Optical networking technologies that will create future bandwidth abundant networks," J. Opt. Commun. Netw., vol.1, no.2, pp.A81–A93, July 2009.

[4] H. Hasegawa and K. Sato, "Hierarchical optical path network design for future peta-bit class networks," Proc. OptoElectronics and Communications Conference, pp.734–735, July 2010.

[5] X. Cao, V. Anand, Y. Xiong, and C. Qiao, "A study of waveband switching with multilayer multigranular optical cross-connects," IEEE J. Sel. Areas Commun., vol.21, no.7, pp.1081–1094, Sept. 2003.

[6] Y. Yamada, H. Hasegawa, and K. Sato, "Hierarchical optical path network design algorithm considering waveband protection," J. Lightwave Technol., vol.27, no.24, pp.5736–5748, Dec. 2010.

[7] I. Yagyu, H. Hasegawa, and K. Sato, "An efficient hierarchical optical path network design algorithm based on traffic demand expression in a Cartesian produce space," IEEE J. Sel. Areas Commun., vol.26, no.6, pp.22–31, Aug. 2008.

[8] M. Lee, J. Yu, Y. Kim, C. Kang, and J. Park, "Design of hierarchical crossconnect WDM networks employing a two-stage multiplexing scheme of waveband and wavelength," IEEE J. Sel. Areas Commun., vol.20, no.1, pp.166–171, Jan. 2002.

[9] S. Kakehashi, H. Hasegawa, and K. Sato, "Optical cross-connect switch architectures for hierarchical optical path network," IEICE Trans. Commun., vol.E91-B, no.10, pp.3174–3184, Oct. 2008.

[10] S. Mitsui, H. Hasegawa, and K. Sato, "Demonstration of compact hierarchical optical path cross-connect utilizing wavelength/waveband selective switches," Proc. Opt. Fiber Commun. Conf. and Exposition and The National Fiber Optic Engineers Conf., NThF4, March 2010.

[11] P. Wall, P. Colbourne, C. Reimer, and S. McLaughlin, "WSS switching engine technologies," Proc. Opt. Fiber Commun. Conference and Exposition and The National Fiber Optic Engineers Conf., OWC1, Feb. 2008.

[12] M. Yano, F. Yamagashi, and T. Tsuda, "Optical MEMS for photonic switching — Compact and stable optical crossconnect switches for, simple, fast, and flexible wavelength applications in recent photonic networks," IEEE J. Sel. Top. Quantum Electron., vol.11, no.2, pp.383–394, March/April 2005.

[13] K. Ishii, H. Hasegawa, K. Sato, M. Okuno, S. Kamei, and H. Takahashi, "An ultra-compact waveband cross-connect switch module to create cost-effective multi-degree reconfigurable optical node," Proc. Eur. Conf. Optical Commun., paper 4.2.2, Sept. 2009.

[14] M. Okuno, K. Kato, R. Nagase, A. Himeno, Y. Ohmori, and M. Kawachi, "Silica-based 8×8 optical matrix switch integrating new switching units with large fabrication tolerance," J. Lightwave Technol., vol.17, no.5, pp.771–781, May 1999.

[15] T. Goh, M. Yasu, K. Hattori, A. Himeno, M. Okuno, and Y. Ohmori, "Low loss and high extinction ratio strictly nonblocking 16×16 thermooptic matrix switch on 6-in wafer using silica-based planar lightwave circuit technology," J. Lightwave Technol., vol.19, no.3, pp.371–379, March 2001.

[16] H.C. Le, H. Hasegawa, and K. Sato, "Hierarchical optical path network design algorithm considering waveband add/drop ratio constraint," Proc. International Conf. on Opt. Internet, C-16-AM2-1, Oct. 2008.

[17] H.C. Le, H. Hasegawa, and K. Sato, "Hierarchical optical path network design algorithm considering waveband add/drop ratio constraint," J. Opt. Commun. Netw., vol.2, no.10, pp.872–882, Oct. 2010.

[18] H.C. Le, H. Hasegawa, and K. Sato, "Hierarchical optical path network design algorithm that can best utilize WSS/WBSS based cross-connects," Proc. International Conf. on Photonics in Switching, ThII2-3, Sept. 2009.

[19] K. Ishii, O. Moriwaki, H. Hasegawa, K. Sato, Y. Jinnouchi, M. Okuno, and H. Takahashi, "Development of hierarchical optical cross-connect system for ROADM-ring connection using PLC technologies," IEEE Photonics Technol. Lett., vol.22, no.7, pp.498–500, April 2010.

[20] L.E. Nelson, S.L. Woodward, P.D. Magill, S. Foo, M. Moyer, and M. O'Sullivan, "Real-time detection of a 40 Gbps intradyne channel in the presence of multiple received WDM channels," Proc. Opt. Fiber Commun. Conference and Exposition and The National Fiber Optic Engineers Conf., March 2010.

[21] R. Hirako, K. Ishii, H. Hasegawa, and K. Sato, "Development of compact hierarchical optical path cross-connect prototype utilizing integrated colorless multi/demultiplexers," Proc. Eur. Conf. Optical Commun., We.8.A.5, Sept. 2010.

[22] J.P. Vasseur, M. Pickavet, and P. Demeester, Network Recovery, Elsevier, 2004.

[23] R.A. Spanke, "Architectures for guided-wave optical space switching systems," IEEE Commun. Mag., vol.25, no.5, pp.42–48, May 1987.

[24] K. Sato, Advances in Transport Network Technologies: Photonic networks, ATM, and SDH, Artech House, Norwood, 1996.

[25] P. Ghelfi, F. Cugini, L. Poti, A. Bogoni, P. Castoldi, R.D. Muro, and B. Nayar, "Optical cross connect architecture with per-node add/drop functionality," Proc. Opt. Fiber Commun. Conference and Exposition and The National Fiber Optic Engineers Conf., NTuC3, March 2007.

[26] P. Roorda and B. Collings, "Evolution to colorless and directionless ROADM," Proc. Opt. Fiber Commun. Conference and Exposition and The National Fiber Optic Engineers Conf., NWE2, Feb. 2008.

[27] S.L. Woodward, M.D. Feuer, P. Palacharla, X. Wang, I. Kim, and D. Bihon, "Intra-node contention in a dynamic, colorless, nondirectional ROADM," Proc. Opt. Fiber Commun. Conference and Exposition and The National Fiber Optic Engineers Conf., PDPC8, March 2010.

[28] K. Sato, "Are all optical networks manageable?," Opt. Fiber Commun. Conference and Exposition and The National Fiber Optic Engineers Conf., Workshop OMF, March 2010.

[29] ITU-T Recommendation G.709/Y.1331 (12/2009), Interfaces for the optical transport network (OTN).

[30] L. Blair and S. Thiagarajan, "Impact of moving to 100 Gbps on the cost per bit of a USA national network," Proc. Opt. Fiber Commun. Conference and Exposition and The National Fiber Optic Engineers Conf., NME4, March 2010.

[31] Y. Yamada, H. Hasegawa, and K. Sato, "Coarse granular routing in optical path networks and impact of supplemental intermediate grooming," Proc. Eur. Conf. Optical Commun., Th.10.G1, Sept. 2010.

Appendix

Table A· 1 Formulation for switch scale.

Figure	Switch scale
Figure1	$K^2L^2(1+x)^2$
Figure2	$K^2L(1+x)^2$
Figure3	$4K^2M+2yK^2M^2+4y^2K^2M^2N^2$
Figure4	$K^2M+2yK^2M^2+y^2K^2M^2N+2yKMN$

K : number of fiber
M : number of waveband paths per fiber
N : number of wavelength paths per waveband path
L : number of wavelength paths per fiber
x : ratio of ratio of wavelength paths to be added/dropped for connections to electrical systems to those coming /outgoing to/from the node
y :ratio of wavebands that are added from WXC to WBXC, to wavebands that are launched from the node
z : ratio of wavelength paths that are added from electrical systems to WXC, to the wavelength paths that are added from WXC to WBXC

Ryosuke Hirako was born in 1987. He graduated from the Nagoya University, department of ECCS in 2009 and is now a graduate student of the department. His major interests include photonic network node architectures, waveband routing devices, and optical performances.

Kiyo Ishii received M.E. degree in electrical and electronic engineering and computer science from the Nagoya University, Nagoya, Japan, in 2008. Currently she is a Research Fellow of the Japan Society for the Promotion of Science, as well as a Ph.D. student at Nagoya University. She is currently pursuing both node systems and network designs to develop hierarchical optical path networks that are large-capacity, highly reliable, and low-power-consumption.

Hiroshi Hasegawa received the B.E., M.E., and D.E. degrees all in Electrical and Electronic Engineering from the Tokyo Institute of Technology, Tokyo, Japan, in 1995, 1997, and 2000, respectively. From 2000 to 2005, he was an assistant professor of the Department of Communications and Integrated Systems, Tokyo Institute of Technology. Currently he is an associate professor of Nagoya University. His current research interests include Photonic Networks, Image Processing (especially Super-resolution), Multidimensional Digital Signal Processing and Time-Frequency Analysis. He received the Young Researcher Awards from SITA (Society of Information Theory and its Applications) and IEICE (Institute of Electronics, Information and Communication Engineers) in 2003 and 2005, respectively. Dr. Hasegawa is a member of SITA and IEEE.

Ken-ichi Sato is currently a professor at the graduate school of Engineering, Nagoya University, and he is an NTT R&D Fellow. Before joining the university in April 2004, he was an executive manager of the Photonic Transport Network Laboratory at NTT. His R&D activities covers future transport network architectures, network design, OA&M (operation administration and maintenance) systems, photonic network systems including optical cross-connect/ADM and photonic IP routers, and optical transmission technologies. He has authored/co-authored more than 300 research publications in international journals and conferences. He holds 35 granted patents and more than 100 pending patents. He received his B.S., M.S., and Ph.D. degrees in electronics engineering from the University of Tokyo, Tokyo, Japan, in 1976, 1978, and 1986, respectively. He received the Young Engineer Award in 1984, the Excellent Paper Award in 1991, and the Achievement Award in 2000 from the Institute of Electronics, Information and Communication Engineers (IEICE) of JAPAN, and the best paper awards in 2007 and 2008 from the IEICE Communications Society. He was also the recipient of the distinguished achievement Award of the Ministry of Education, Science and Culture in 2002. His contributions to ATM (Asynchronous Transfer Mode) and optical network technology development extend to co-editing three IEEE JSAC special issues and the IEEE JLT special issue once, organizing several Workshops and Conference technical sessions, serving on numerous committees of international conferences including OFC and ECOC, authoring a book, Advances in Transport Network Technologies (Artech House, 1996), and co-authoring thirteen other books. He is a Fellow of the IEEE.

Osamu Moriwaki was born in Tokyo, Japan, in 1975. He received the B.E. and M.E. degrees in electrical engineering, from the University of Tokyo, Tokyo, Japan in 1998 and 2000, respectively. He joined NTT Photonics Laboratories, Japan, in 2000, where he has been engaged in research on wavelength routing devices. Mr. Moriwaki is a member of the IEEE Photonics Society.